CELLULAR UPTAKE AND TOXICITY OF GOLD NANOPARTICLES IN A TUMOR-LIKE (HYPOXIC) ENVIRONMENT

By

Mehrnoosh Neshatian

A thesis
Presented to Ryerson University
in partial fulfillment of the
requirements for the degree of
Master of Science
in the Program of
Biomedical Physics

Toronto, Ontario, Canada, 2015

Author's Declaration

I hereby declare that I am the sole author of this thesis. This is a true copy of the thesis, including any required final revisions as accepted by my examiners.

I authorize Ryerson University to lend this thesis to other institutions or individuals for the purpose of scholarly research.

I further authorize Ryerson University to reproduce this thesis by photocopying or by other means, in total or in part, at the request of other institutions or individuals for the purpose of scholarly research.

I understand that my thesis may be made electronically available to the public.

Mehrnoosh Neshatian

Abstract

Cellular Uptake and Toxicity of Gold Nanoparticles in a Tumor-Like (Hypoxic) Environment

Mehrnoosh Neshatian

Master of Science, Biomedical Physics

Ryerson University, 2015

Cancer cells deprived adequate oxygen tension, are called hypoxic cells. Hypoxic shows resistance to both chemotherapy and/or radiotherapy. On the other hand gold Nanoparticles (GNPs) are being used as promising agents in cancer therapy. GNPs can be used as radiosensitizer and drug carrier agents. It also has been shown that uptake of GNPs in normal oxygenated (normoxic) cancer cells is maximum for 50 nm GNPs. However, it is important to know the variation in GNPs uptake and toxicity of 50 nm particles in a tumor-like (hypoxic) environment. Hence, we have investigated toxicity and uptake of 50 nm GNPs in hypoxic cancer cells.

MCF-7 (breast cancer cell line) and HeLa (cervical cancer cell line), were used in this study. The results of this study showed that uptake of GNPs in hypoxic cells were dependent on the exposure duration to hypoxic conditions. Cancer cells under prolong hypoxia showed highest GNPs uptake.

Acknowledgements

First, I would like to express my gratitude towards my supervisor, Dr. Devika Chithrani, for her encouragement and support. She made me believe in my skills and abilities. Furthermore, I would like to thank her for being a good friend to me when I needed one.

Secondly, I would like to express my gratitude towards my committee members Dr. Michael Kolios and Dr.Yuan Xu for their guidance throughout my thesis.

Thirdly, I would like to extend my appreciation to Dr. Bradly Wouters and Stephen Chung for providing me with the instruments necessary for my hypoxia experiments. Furthermore, I would like to thank my lab members, Celina Yang, Charmainne Cruje, and Darren Yohan for their help and suggestions.

Last but not least, I would like to express my gratitude towards my family for their constant support and affection and to my husband for providing constant motivation and for being my rock throughout the hardest time in the past year.

Table of Contents

List of Tables

List of Figures

Symbols & Abbreviations

AAS – Atomic absorption spectroscopy

ATP – Adenosine triphosphate

DLS – Dynamic light scattering

FBS - Fetal bovine serum

FTIR - Fourier transform infrared spectroscopy

GNP – Gold nanoparticle

HIF – Hypoxia inducible factor

ICP-AES – Inductively coupled plasma – Atomic emission spectroscopy

NP – Nanoparticle

OXPHOS – Oxidative phosphorylation

SAM – Spectral angle mapping

SD – Standard deviation

SE – Standard error

TEM – Transmission electron microscope

1 Introduction

1.1 Background and Motivation

Hypoxia exists in most solid tumors and is heterogeneous. It is associated with poor prognosis according to its contribution to chemoresistance, radio resistance, invasiveness, and metastasis and cell death resistance [1-4]. Hence, the understanding of tumor hypoxia is often desired in oncology. However, in the era of nanotechnology, nanomedicine has shown promising applications in both diagnostic and therapeutic. Nano-scale agents are being explored for targeted therapeutics and imaging in medicine, particularly in cancer therapy. GNPs have been introduced as a versatile platform for biomedical research, due to the favorable physical and chemical properties along with its biocompatibility and ease of fabrication. This led to the use of GNPs in cellular imaging, targeted drug and gene delivery, biosensing, cancer diagnosis and treatment. GNPs have also been explored as a radiation dose enhancer in radiation therapy and as a drug carrier in chemotherapy. However, as explained previously, the therapeutic effects can be varied under different oxygen levels. Hence, we believe that GNPs can be used as a model NP system to map the variation of GNPs uptake in cancer cells under hypoxic conditions. Hence, in this study, the uptake of GNPs in hypoxic cells was investigated as a function of hypoxia severity.

1.2 Introduction to Hypoxia

1.2.1 Oxygen Effects on Cell Metabolism

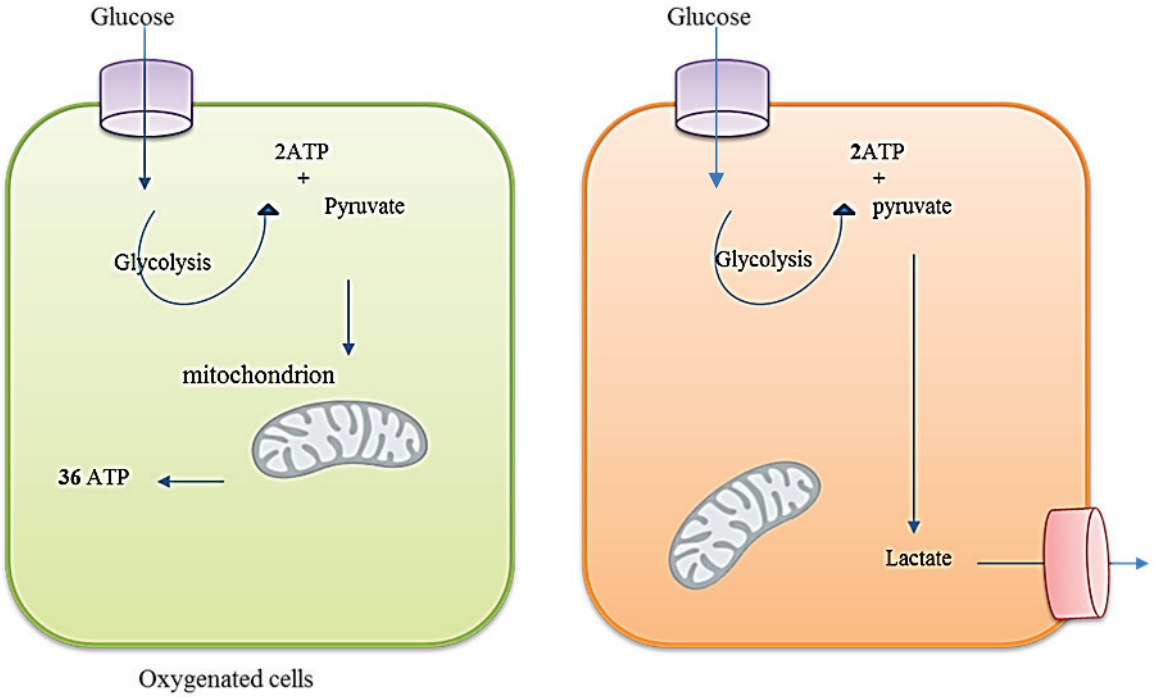

<Figure 1.1> Schematic of a glucose metabolism in a cell under normoxia and hypoxia. The left and right figures explain the energy generation in a normoxic and hypoxic cell, respectively. Normoxic and hypoxic cells generate 36 and 2 ATP molecules per glucose, respectively.

One of the most significant roles of oxygen in living species is generating energy from glucose. When glucose enters a living cell, it undergoes a series of metabolic reactions resulting in 2 ATPs (adenosine triphosphate) and a pyruvate molecule. In the presence of oxygen, a pyruvate molecule enters Krebs cycle (an energy generating cycle which occurs in the mitochondrion). This results in 36 more ATPs. However, in the absence of oxygen, the pyruvate molecule

converts to lactate and leaves the cell. In the presence of oxygen, cells can generate 18 times more ATPs per glucose molecule, as compared to cells under hypoxic conditions [5, 6].

1.2.2 Normoxia vs. Hypoxia

In complex multicellular organisms, oxygen is mainly transported throughout the body *via* the respiratory system. When oxygen enters the body *via* airways, the oxygen partial pressure is approximately 160 mm Hg to 100 mm Hg. This pressure drops to 60 mm Hg to 5 mm Hg as oxygen transports through blood vessels to tissues and cells. It is known that oxygen partial pressure is kept to a threshold where cellular biological functions are normally maintained. The threshold level of oxygen for proper functioning of the cell is approximately 5 mm Hg (0.7% O_2 in the gas phase). Cellular behavior varies if oxygen partial pressure decreases. The cells which receive oxygen below the threshold level are known as hypoxic cells [2, 7].

1.2.3 Tumor Hypoxia

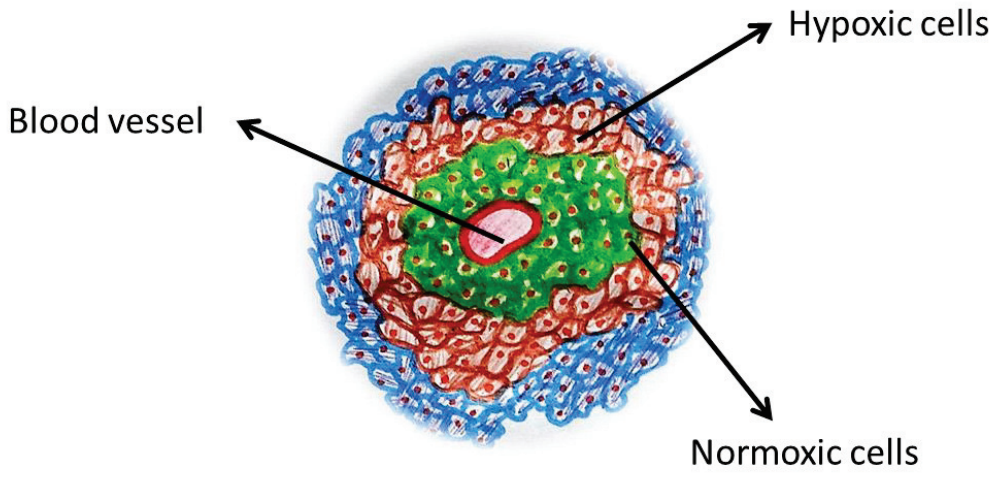

<Figure 1.2> Tumor hypoxia. A schematic representing the generation of hypoxic cells. Cells that are further from blood vessel have lower oxygen available and become hypoxic.

More than 90% of cancers consist of solid tumors [2]. Almost 60 years ago, Thomlinson and Grey observed that hypoxic regions develop within a tumor. In their experiment, they noticed that there was more necrosis farther from blood vessels [8]. Tumor cells are known to be fast proliferating which results in the high demand of oxygen and nutrients. However, the vascularization rate does not follow what is necessary for the fast proliferating cells. Hence, the angiogenesis signal is activated and new capillaries are formed in order to deliver oxygen and nutrients to these tumor cells. However, these newly formed microvessels surrounding the tumor are different from the vasculature in normal tissues. Thus, it is known that in solid tumors, oxygen delivery to the cells is usually reduced or even suppressed due to severe structural abnormalities of tumor microvessels [9, 10]. This type of hypoxia is called chronic or diffusion-limited hypoxia. Furthermore, there is another type of hypoxia called perfusion-limited or acute hypoxia. This type of hypoxia occurs due to temporary blockage of blood vessels [11].

1.2.4 Metabolism in Hypoxic Cells

Hypoxic cancer cells undergo two metabolic challenges due to the microenvironment with low oxygen tension. First, a strategy to provide cells with sufficient energy for proliferation and growth must be developed. Secondly, an adaptive pathway to stay alive must be found [12].

To overcome these metabolic stresses, a hypoxic transcription factor, HIF (Hypoxia Inducible Factor), is activated to alter the metabolism of hypoxic cells. As a result of HIF activation, hypoxic cancer cells shift from oxygen consuming ATP production (oxidative phosphorylation - OXPHOS) to anaerobic glycolysis (involves no oxygen). This is a less efficient way for ATP generation. Hence, hypoxic cancer cells utilize glucose inefficiently, thus causing more glucose intake to compensate for energy needed for growth and survival. HIF is also responsible for the

over-expression of glucose transporters, Glut1 and Glut3. These glucose transporters are required to assure efficient glucose intake if glucose resources are limited [13, 14].

1.3 Hypoxia and Therapy

1.3.1 Hypoxia and Radiation Therapy

The availability of oxygen in an intracellular environment is one of the characteristics that affect the radiation outcome. Ionization radiation used in radiation therapy produces free radicals, near or on DNA. These free radicals then tend to oxidize and produce DNA strand breaks and induce cell apoptosis. However, at low oxygen content, free radicals are reduced by sulfhydryl groups (–SH groups), which leaves DNA without damages and cell continue to proliferate. Hence, for achieving equivalent cell death for tumor with hypoxia, the radiation dose should be raised by 2.5 to 3 folds for a single fraction of radiation [14, 15].

Several clinical studies have shown that radiation therapy is more successful for patients with less or no hypoxic regions in tumors as compared to severe hypoxic tumors [1, 16, 17].

1.3.2 Hypoxia and Chemotherapy

Chemotherapy is less effective when hypoxic regions are present in the tumor since certain drugs, such as Bleomycin, cause damage to DNA similar to radiation therapy [18]. Certain drugs cannot reach hypoxic regions due to their distance from vasculature In addition, the uptake of certain drugs decreases in an acidic microenvironment around hypoxic regions [19]. Furthermore, there is evidence that shows hypoxia is responsible for upregulation of genes, which affect drug resistance [20].

1.4 Gold Nanoparticles

1.4.1 GNPs and Cancer therapy

GNPs are being used as a radiation dose enhancer and as an anticancer drug carrier in cancer therapy. Several *in vivo* and *in vitro* studies have shown promising results for GNPs used as a favorable agent in cancer therapy. For example, GNPs were used to effectively carry the anticancer drug, doxorubicin, to overcome multidrug resistance in cancer cells [20]. Gold nanoshells were also used as a photothermal therapy agent. It was found that temperature of treated cells increased by 37℃, whereas temperature increment was 9℃ in the control group [21]. In addition, several studies have shown the effect of radiosentization due to GNPs. It was recently shown that the nuclear targeting of cancer cells with peptide-coated GNPs could increase the radiation dose enhancement by a factor of four [22].

1.4.2 Regular Pathway of GNPs in Cells

It has been shown that Receptor-Mediated Endocytosis (RME) is mostly responsible for the uptake of GNPs in cells [23-27]. It is known that RME pathway is an energy dependent process [28, 29]. When GNPs attach to the receptors on the cell membrane, cell membrane wraps around these particles to initiate internalization through the endocytosis process. GNPs localized in endosomes fuse with lysosomes to process their content. Once processed, GNPs are excreted from the cell *via* the exocytosis process [29]. A schematic of RME pathway can be found in **Figure 1.3.**

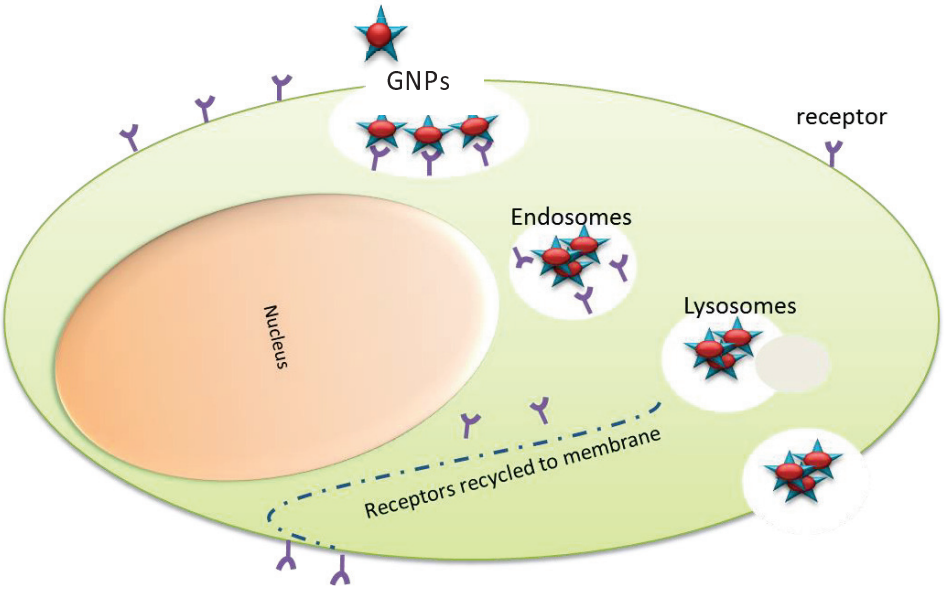

<Figure 1.3> Regular pathway of GNPs in cells. As illustrated in the schematic, GNPs enters the cell *via* a receptor mediated endocytosis process. GNPs gets trapped in endosomes and fused with lysosomes for processing. At the end of the process, GNPs get excreted from the cell *via* exocytosis process.

1.5 Hypothesis and Specific Objectives

This study is based on the hypothesis that GNPs are non-toxic to hypoxic cells. Furthermore, we believe that the uptake of GNPs in cancer cells varies in noromxic compare to hypoxic cells and extent of this difference depends on the exposure time of hypoxic cells to hypoxic environment.

The specific objectives are:

- To investigate the cellular toxicity of GNPs in a hypoxic environment
- To investigate the difference in GNP uptake in hypoxic cells as compared to normoxic cells
- To invastigate GNP uptake in hypoxic cells as a function of the exposure time to hypoxic conditions

1.6 References

1. Brizel, D. M., Scully, S. P., Harrelson, J. M., Layfield, L. J., Bean, J. M., Prosnitz, L. R., & Dewhirst, M. W. (1996). Tumor oxygenation predicts for the likelihood of distant metastases in human soft tissue sarcoma. *Cancer research*, *56*(5), 941-943.

2. Brown, J. M. (2000). Exploiting the hypoxic cancer cell: mechanisms and therapeutic strategies. *Molecular medicine today*, *6*(4), 157-162.

3. Dang, C. V., & Semenza, G. L. (1999). Oncogenic alterations of metabolism. *Trends in biochemical sciences*, *24*(2), 68-72.

4. Moeller, B. J., Richardson, R. A., & Dewhirst, M. W. (2007). Hypoxia and radiotherapy: opportunities for improved outcomes in cancer treatment. *Cancer and Metastasis Reviews*, *26*(2), 241-248.

5. Dang, C. V., & Semenza, G. L. (1999). Oncogenic alterations of metabolism. *Trends in biochemical sciences*, *24*(2), 68-72.

6. Porporato, P. E., Dhup, S., Dadhich, R. K., Copetti, T., & Sonveaux, P. (2011). Anticancer targets in the glycolytic metabolism of tumors: a comprehensive review. *Frontiers in pharmacology*, *2,* 1-18.

7. Lee, K., Roth, R. A., & LaPres, J. J. (2007). Hypoxia, drug therapy and toxicity. *Pharmacology & therapeutics*, *113*(2), 229-246.

8. Thomlinson, R. H., & Gray, L. H. (1955). The histological structure of some human lung cancers and the possible implications for radiotherapy. *British journal of cancer*, *9*(4), 539-549.

9. Vaupel, P., F. Kallinowski, and P. Okunieff. (1990). Blood flow, oxygen consumption and tissue oxygenation of human tumors. *Oxygen Transport to Tissue XII*. Springer US, 895-905.

10. Liao, D., & Johnson, R. S. (2007). Hypoxia: a key regulator of angiogenesis in cancer. *Cancer and Metastasis Reviews*, *26*(2), 281-290.

11. Brown, J. M., & Giaccia, A. J. (1998). The unique physiology of solid tumors: opportunities (and problems) for cancer therapy. *Cancer research*, *58*(7), 1408-1416.

12. Jones, R. G., & Thompson, C. B. (2009). Tumor suppressors and cell metabolism: a recipe for cancer growth. *Genes & development*, *23*(5), 537-548.

13. Ebert, B., Gleadle, J., O'Rourke, J., Bartlett, S., Poulton, J., & Ratcliffe, P. (1996). Isoenzyme-specific regulation of genes involved in energy metabolism by hypoxia: similarities with the regulation of erythropoietin. *Biochemical Journal*, *313*, 809-814.

14. Brown, J. M., & Wilson, W. R. (2004). Exploiting tumour hypoxia in cancer treatment. *Nature Reviews Cancer*, *4*(6), 437-447.

15. Harrison, L. B., Chadha, M., Hill, R. J., Hu, K., & Shasha, D. (2002). Impact of tumor hypoxia and anemia on radiation therapy outcomes. *The Oncologist*, *7*(6), 492-508.

16. Nordsmark, M., Bentzen, S. M., Rudat, V., Brizel, D., Lartigau, E., Stadler, P, Overgaard, J. (2005). Prognostic value of tumor oxygenation in 397 head and neck tumors after primary radiation therapy. An international multi-center study. *Radiotherapy and Oncology*, *77*(1), 18-24.

17. Gee, H. E., Camps, C., Buffa, F. M., Patiar, S., Winter, S. C., Betts, G., Harris, A. L. (2010). hsa-miR-210 is a marker of tumor hypoxia and a prognostic factor in head and neck cancer. *Cancer*, *116*(9), 2148-2158.

18. Teicher, B. A., Lazo, J. S., & Sartorelli, A. C. (1981). Classification of antineoplastic agents by their selective toxicities toward oxygenated and hypoxic tumor cells. *Cancer research*, *41*(1), 73-81.

19. Gerweck, L. E., Kozin, S. V., & Stocks, S. J. (1999). The pH partition theory predicts the accumulation and toxicity of doxorubicin in normal and low-pH-adapted cells. *British journal of cancer*, *79*(5-6), 838-842.

20. Wang, F., Wang, Y. C., Dou, S., Xiong, M. H., Sun, T. M., & Wang, J. (2011). Doxorubicin-tethered responsive gold nanoparticles facilitate intracellular drug delivery for overcoming multidrug resistance in cancer cells. *ACS nano*, *5*(5), 3679-3692.

21. Hirsch, L., Stafford, R. J., Bankson, J. A., Sershen, S. R., Rivera, B., Price, R. E, West, J. L. (2003). Nanoshell-mediated near-infrared thermal therapy of tumors under magnetic resonance guidance. *Proceedings of the National Academy of Sciences*, *100*(23), 13549-13554.

22. Yang, C., Neshatian, M., van Prooijen, M., & Chithrani, D. B. (2014). Cancer Nanotechnology: Enhanced Therapeutic Response Using Peptide-Modified Gold Nanoparticles. *Journal of nanoscience and nanotechnology*, *14*(7), 4813-4819.

23. Jin, H., Heller, D. A., Sharma, R., & Strano, M. S. (2009). Size-dependent cellular uptake and expulsion of single-walled carbon nanotubes: single particle tracking and a generic uptake model for nanoparticles. *Acs Nano*, *3*(1), 149-158.

24. Kirchhausen, T. (2000). Three ways to make a vesicle. *Nature Reviews Molecular Cell Biology*, *1*(3), 187-198.

25. Chithrani, B. D., Ghazani, A. A., & Chan, W. C. (2006). Determining the size and shape dependence of gold nanoparticle uptake into mammalian cells. *Nano letters*, *6*(4), 662-668.

26. Kam, N. W. S., Liu, Z., & Dai, H. (2006). Carbon nanotubes as intracellular transporters for proteins and DNA: an investigation of the uptake mechanism and pathway. *Angewandte Chemie*, *118*(4), 591-595.

27. Kim, J. S., Yoon, T. J., Yu, K. N., Noh, M. S., Woo, M., Kim, B. G. & Cho, M. H. (2006). Cellular uptake of magnetic nanoparticle is mediated through energy-dependent endocytosis in A549 cells. *Journal of veterinary science*, *7*(4), 321-326.

28. Chithrani, B. D., & Chan, W. C. (2007). Elucidating the mechanism of cellular uptake and removal of protein-coated gold nanoparticles of different sizes and shapes. *Nano letters*, *7*(6), 1542-1550.

29. Kneipp, J., Kneipp, H., McLaughlin, M., Brown, D., & Kneipp, K. (2006). In vivo molecular probing of cellular compartments with gold nanoparticles and nanoaggregates. *Nano Letters*, *6*(10), 2225-2231.

2 Uptake of Gold Nanoparticles in Breathless (Hypoxic) Cancer Cells

Mehrnoosh Neshatian[1] MSc, Stephen Chung[2] BSc, Darren Yohan[1] BSc, Celina Yang[1] BSc, and Devika B. Chithrani[1]* PhD

Abstract

Gold nanoparticles (GNPs) are emerging as promising novel agents for cancer therapy. However, the oxygen concentration in human tumors is highly heterogeneous, and there are many regions with very low levels of oxygen (hypoxia). A majority of solid tumors contain regions with oxygen pressure values of less than 0.7% in the gas phase. The purpose of this study was to investigate NP stability, toxicity, and cellular uptake under hypoxic conditions. GNPs 50 nm in diameter was used, and the experiment was performed under 0.2% (hypoxic) and 21% (normoxic) oxygen levels using MCF-7 and HeLa cells. Hypoxic cells with prolonged exposure (eighteen hours) to hypoxia had a higher NP uptake at both 6- and 24-hour NP incubation time points. No significant toxicity was introduced by NPs under hypoxic and normoxic conditions. These findings contribute vital role in the optimization of GNP-based therapeutics in cancer treatment.

2.1 Background

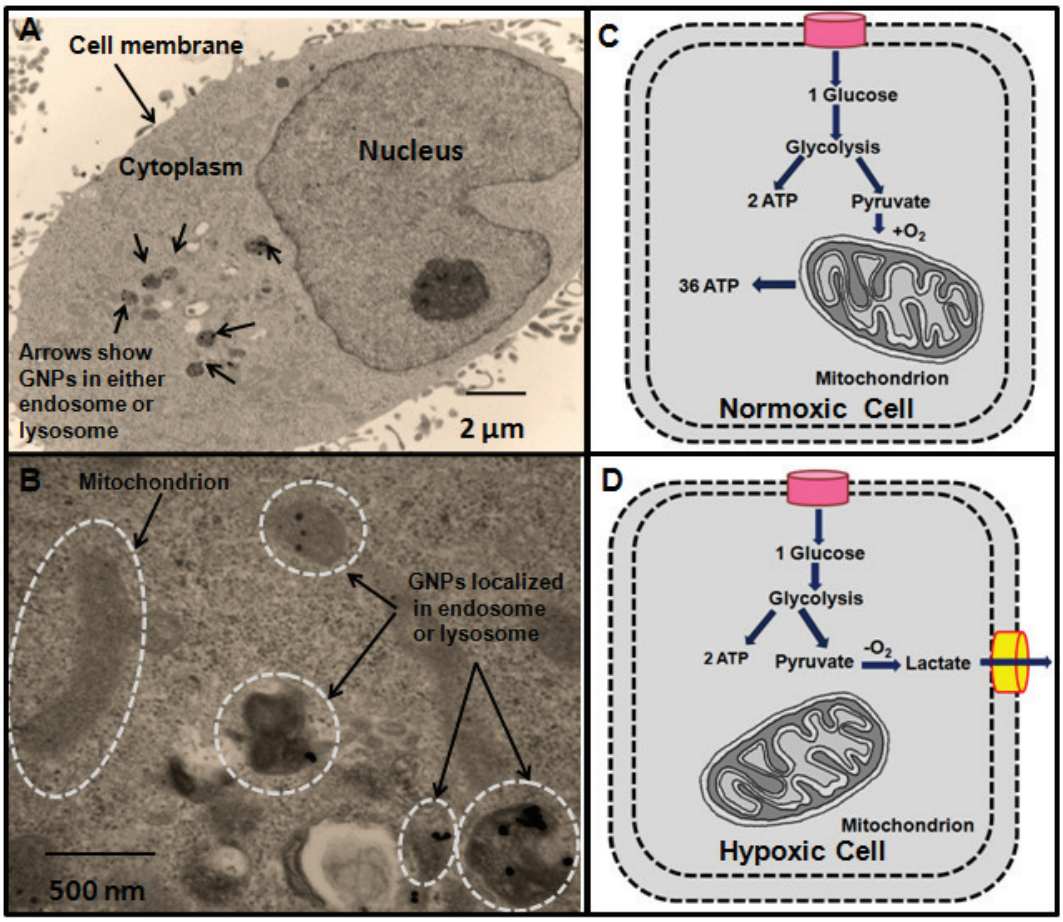

<Figure. 2.1> The metabolic difference between normoxic and hypoxic cells. (A) A cross-sectional TEM image of a cell with internalized GNPs. (B) An illustrated TEM image of a small section of a cell showing a mitochondrion and vesicles with internalized GNPs. (C) A normoxic cell primarily metabolizes glucose to pyruvate, followed by the complete oxidation of pyruvate to CO_2 in the mitochondria, generating 36 ATP molecules per glucose molecule. (B) A hypoxic cell has limited O_2, and pyruvate is metabolized to lactate generating 2 ATP molecules per glucose molecule.

Recent progress in the usage of nanotechnology for biomedical research has led to the rapid development of novel materials known as “nanoparticles” (NPs) for improved therapeutics and imaging in cancer therapy [1–4]. Cancer nanotechnology allows the further development of safer and more effective diagnostic and therapeutic modalities for cancer therapy [2, 3, 5–7]. The ultimate

or fundamental goal of nanoparticle (NP)-based platforms is the successful targeted delivery and monitoring of therapeutics to tumors while causing minimal damage to normal tissue and minimal side effects to the patient. Among other NPs, GNPs are being explored as a model NP system for cancer research because (a) their size, shape, and surface properties can be easily tailored, (b) they appear to be biocompatible and have limited toxicity, and (c) they can be used as a radiosensitizer and drug carrier in cancer therapy [1, 3]. Previous *in vitro* studies have demonstrated that GNPs are capable of being used as radiosensitizers in cancer therapy [8–10]. The GNPs used in those studies were localized in organelles, such as the endosomes and lysosomes, in the cytoplasm of cancer cells (as illustrated in **Figures. 2.1(A), (B)**) [8, 11]. One study recently showed that the targeting of GNPs into the nucleus of cancer cells improved the radiation dose enhancement by a factor of four [12]. Most of these studies were performed with properly oxygenated (normoxic) cells. The cells in a solid tumor grow very fast and the vasculature, which supplies oxygen and nutrients to the tissues, is unable to meet the demand of the rapidly growing tumor cells. This lack of oxygen and nutrients results in the activation of angiogenesis signals to form new capillaries for the delivery of oxygen and nutrients to these rapidly growing cells [13, 14]. However, this newly formed vasculature around the tumor greatly differs from the vasculature in normal tissue in both structure and function. This variation includes abnormal vessel walls, leakiness, abnormal vascular architecture, and abnormal density. Abnormal tumor vasculature causes poor blood flow through the tumor regions and leaves some of these regions hypoxic [13, 15]. Tumor hypoxia usually occurs at distance of 100–200 μm from blood vessels [16–19]. Jain and colleagues have used a combination of fluorescence ratio imaging and phosphorescence quenching microscopy (high resolution; ≤ 10 μm) to measure O_2 concentration profiles around blood vessels in a human tumor xenograft [16]. Tannock and colleagues have used

immunofluorescence to map the hypoxic regions around tumor blood vessels [19]. Researchers have been able to make accurate measurements of O_2 levels in tumors using a commercially available oxygen electrode (the Eppendorf electrode) [20]. It has been found that the majority of solid tumors contain regions with O_2 pressure values of less than 5 mm Hg (corresponding to approximately 0.7% O_2 in the gas phase or 7 μM in the solution), while the partial pressure of oxygen of normal tissues is approximately 30–50 mm Hg (corresponding to approximately 4–7% O_2 in the gas phase) [21]. Hence, most solid human tumors have cells that do not receive enough oxygen, and these cells are known as hypoxic cells [21–24]. These cells develop adaptive responses to survive and proliferate under hypoxic conditions. Under hypoxia, ATP generation shifts from the phosphorylation pathway in the mitochondrion to the oxygen-independent pathway of glycolysis[25, 26]. A transmission electron micrograph (TEM) in **Figure 2.1(B)** shows a cross-sectional image of a mitochondrion. Although ATP can be generated faster through a glycolysis pathway compared to oxidative phosphorylation, it is less efficient when comparing amounts of ATP produced [25, 27]. As illustrated in **Figure 2.1(C)**, normoxic cells primarily metabolize glucose to pyruvate followed by complete oxidation of pyruvate to CO_2. During this process, 36 ATP molecules are generated in a mitochondrion per glucose molecule. In hypoxic cells, the lack of O_2 results inactivation of the HIF-1 (hypoxia induced factor) pathway for regulation of glucose metabolism [28, 29]. In hypoxic cells, glucose metabolized to 2 ATP molecules and pyruvate leaves the cell in the form of lactate, as illustrated in **Figure 2.1(D)**. For example, a previous study has shown that under hypoxia, alveolar epithelial cells maintain their energy status near that of normoxic cells by increasing anaerobic glycolysis [29]. According to previous research, NPs are internalized, transported across, and removed by cells via an energy dependent process [1, 30.] Hence, it is important to consider the efficacy of treatment in a real tumor-like environment, such

as hypoxia, to further improve NP-based cancer therapeutics. A majority of the previous NP-based work has not taken the hypoxic nature of the tumor microenvironment into consideration. For example, the use of GNPs as a drug carrier, radiation dose enhancer, and as a photothermal agent in cancer therapeutics has been carried out using properly oxygenated cancer cells [3, 4]. Previous studies have shown that NPs of smaller size have a lower uptake compared to larger NPs. NPs 50 nm in size had the highest cell uptake [1, 31–35]. A recent study by Jain et al. showed that smaller NPs (1.9 nm) had a lower uptake in cells pre-exposed to hypoxic conditions (0.1% and 1% O_2) for four hours.36 They incubated the GNPs in hypoxic cells for twenty-four hours before quantifying the NP uptake in the cells. In our study, the cells were pre-exposed to 0.2% hypoxic conditions for a shorter (four hours) or a longer period of time (eighteen hours) before we introduced the NPs. We incubated the NPs for six hours in addition to the twenty-four hour time period. Nanoparticles 50 nm in size were chosen for our study because our previous studies showed that 50 nm NPs had higher uptake in the 10–100 nm size range [31]. In summary, we investigated NP uptake behavior under four different conditions: (a) pre-exposure of cells to hypoxia for four hours followed by incubation with NPs for six hours, (b) pre-exposure of cells to hypoxia for four hours followed by incubation with NPs for 24 hours, (c) pre-exposure of cells to hypoxia for sixteen hours followed by incubation with NPs for six hours, and (d) pre-exposure of cells to hypoxia for eighteen hours followed by incubation with NPs for twenty-four hours. Our results were consistent with a previous study by Jain et al. for the above-mentioned condition “b,” even though our hypoxic conditions deviate from 0.1% to 0.2%. In addition, the stability and toxicity of NPs exposed to prolonged hypoxia were investigated. A proper understanding of NP behavior in hypoxic conditions can be used to understand the outcome of therapeutic treatments in real tumor environments.

2.2 Methods

2.2.1 GNPs Synthesis and Characterization

GNPs 50 nm in diameter was synthesized using the citrate reduction method [31, 37]. First, 300 ml of 1% $HAuCl_4.3H_2O$ was added to 30 ml of double-distilled water and heated on a hot plate whiles stirring. Once it reached the boiling point, 300 µl of 1% Sodium citrate tribasic was added to form GNPs of size 50 nm in diameter. After the colour of the solution changed from dark blue to red, the solution was left to boil for another 5 minutes while stirring. Finally, the GNP solution was brought to room temperature while stirring. GNPs were characterized with Transmission Electron Microscopy (TEM), UV-Visible spectroscopy, Fourier Transform Infrared Spectroscopy (FTIR), and Dynamic Light Scattering (DLS).

2.2.2 TEM Analysis of Cells with Internalized Nanoparticles

Cells incubated with NPs were washed with PBS three times and fixed (2.5% paraformaldehyde, 0.5% glutaraldehyde) for 8 hours. The cells were then post-fixed in 1% osmium tetraoxide for 2 hours, washed and dehydrated in graded concentrations of ethanol (25%, 50%, 70%, and100%) and propylene oxide. Cell samples were then embedded in Epon and thin-sectioned. Thin sections of 60–70 µm were collected on copper grids and stained with a 1:1 mixture of methanol and lead citrate for TEM imaging.

2.2.3 Cell Culture

We used a breast cancer cell line (MCF-7) and a cervical cancer cell line (HeLa) for our study. The cells were cultured in Dulbecco's modified Eagle's medium (DMEM) supplemented with 10% fatal bovine serum (FBS). Cells were incubated at 37°C in a humidified incubator with 95% air/5% CO_2. For cellular uptake studies, the cells were grown in petri dishes (100 mm x 15 mm) until they reached 80% confluence and incubated with fresh medium prior to each incubation experiment with NPs in either normoxic or hypoxic conditions.

2.2.4 Cell Uptake

Cells were seeded with 2.2 $\times 10^6$ density in 10-cm petri culture dishes and were left in a normoxic chamber. When they reached 80% confluence, half of them were moved to the hypoxia chamber and the rest were served as a control group. The cells and GNPs were incubated in the hypoxia chamber separately to reach hypoxic conditions. The hypoxia chamber was gassed under positive pressure with 95% nitrogen, 5% CO_2, and 0.2% O_2. We used two incubation periods of 4 and 18 hours for our experiments. Following the incubation, GNPs were added to the hypoxic cells as well as to the control group. Following 6 and 24 hours of cell incubation with GNPs, cells were washed with PBS three times to remove the GNPs that were not internalized within the cells. The cells were then trypsinized for their removal from the petri dish for quantification purposes.

2.2.5 Quantification

Cells were washed with PBS three times, detached from the petri dish using trypsin, counted, and processed at 120°C in nitric acid for a half hour. The concentration of GNPs was measured using Atomic Absorption Spectroscopy (AAS). The following equations were then used to convert the

number of gold atoms, as determined by AAS, to the number of GNPs. For a sphere of diameter D, the number of atoms (U) in each volume of GNPs was determined. In this calculation, "a" refers to the edge of the unit cell, which has a value of 4.076 Å, and there are four gold atoms per unit cell ($U = (2\pi/3)(D/a)^3$). If M is the measured number of gold atoms from AAS and N is the number of NPs for the analyzed sample ($N = M/U$), the number of NPs per cell can be determined by dividing N by the total number of cells for that sample. This calculation assumes a homogeneous distribution of NPs in the cell population.

2.2.6 Cell Toxicity

HeLa and MCF-7 cells were seeded with 0.02×10^6 cell density in 24-well dishes. The cells were left in the normoxic chamber for their adherence to the bottom. Once adhered to the bottom of the dishes, a group of dishes and a suspension of GNPs were transferred to the hypoxia chamber. After 4 hours, GNPs were added to the one set of dishes in the normoxic and hypoxic chambers. One set of dishes without any added GNPs was used as a control in each chamber. The concentration of GNPs used was 0.6 and 1.2 nMol. We used 0.6 nMol concentration for our cell uptake studies. The cell proliferation was monitored with IncuCyte™ Kinetic Live Cell Imaging System with a 2-hour time interval for 42 hours.

2.2.7 Optical Imaging Using Cytoviva Technology

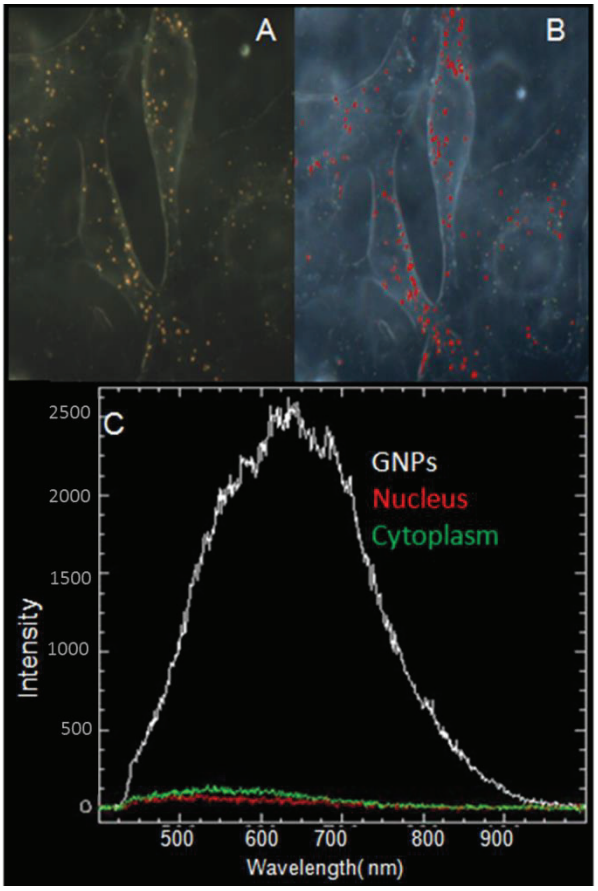

<Figure 2.2> CytoViva hyperspectral imaging of GNPs internalized in cells. (A) The darkfield image of GNPs in cells. (B) The spectral angle map overlaid onto the hyperspectral darkfield image. The spectrum from each pixel is compared with reflectance spectra from GNPs and if a match is determined, the pixels are colored red. (C) The reflectance spectra from one of the GNPs clusters (white line), the background reflectance from the nucleus (red line), and the cytoplasm (green line). The spectra from each pixel in Figure 2.3(B) are compared with these spectra and if a match is determined, the pixels are colored red.

This CytoViva technology was specifically designed for optical observation and spectral confirmation of NPs as they interact with cells and tissues. The illumination of the microscope system utilizes oblique angle illumination to create high signal-to-noise optimized dark field-based images. **Figure 2.2A** is a dark-field image of a group of cells with internalized GNPs. The

GNPs appear bright owing to their high scattering cross-section. With the integrated CytoViva hyperspectral imaging capability, reflectance spectra from specific materials can be captured and measured. The SAM (Spectral Angle Mapping) is an automated procedure used to determine if GNPs are present in the input image, and locates which pixels contain the material in interest. SAM accomplishes these tasks by comparing unknown spectra in hyperspectral imagery with known spectra for the material of interest and in this case it is GNPs. The hyperspectral image shows, the relative degree to which unknown spectra in each image pixel match the known GNP spectrum. **Figure 2.2B** shows the hyperspectral image with an overlaid spectral angle map and the red dots represent GNP clusters. **Figure 2.2C** shows reflectance spectra from one of those red dots and the spectrum (white color) really shows that it is very similar to the reflectance spectrum of GNPs. The background reflectance spectra from the nucleus and cytoplasm are shown and it be clearly seen that the GNP clusters have a very high reflection compared to the background.

2.3 Results

2.3.1 GNPs Characterization

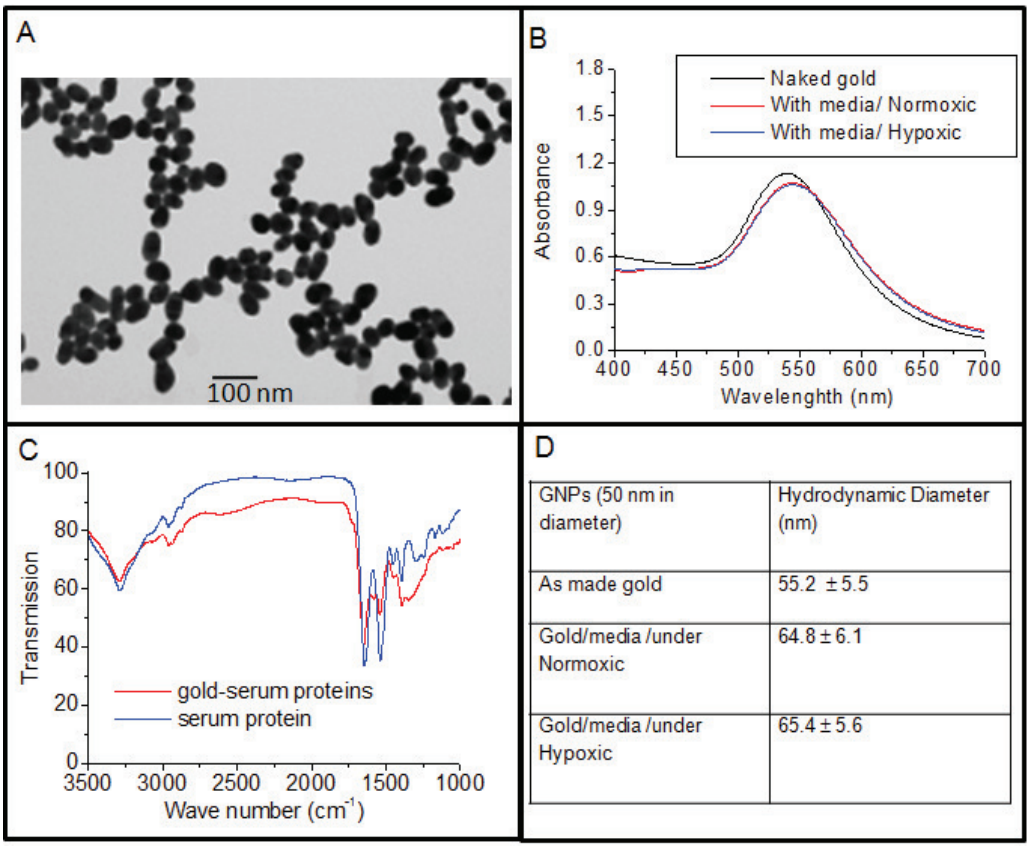

GNPs (50 nm in diameter)	Hydrodynamic Diameter (nm)
As made gold	55.2 ±5.5
Gold/media /under Normoxic	64.8 ± 6.1
Gold/media /under Hypoxic	65.4 ± 5.6

<Figure 2.3> Characterization of GNPs. (A) Transmission electron micrograph of 50 nm diameter GNPs used in the experiment. (B)–(D) UV-visible spectra, FTIR spectra, and hydrodynamic diameter of naked GNPs and GNPs incubated with FBS-supplemented media for 24 hrs in normoxic and hypoxic (0.2% O2) conditions, respectively.

The aim of this work was to elucidate the uptake of GNPs under hypoxia. Our previous studies showed that the GNPs of size 50 nm had the highest uptake and radiation dose enhancement properties among NP sizes between 10-100 nm. Hence, we chose GNPs of size 50 nm for this study. Colloidal GNPs were characterized by UV-Vis spectroscopy, DLS, and TEM imaging. The TEM image in the **Figure 2.3A** shows the naked GNPs. To study the effect of the hypoxic

environment on the stability of NPs, they were kept in a hypoxia chamber for 24 hours. UV-Vis spectroscopy and DLS measurements were performed to investigate the changing characteristics of the NPs. The UV visible spectrum (see **Figure 2.3B**) of GNPs incubated in the media supplemented with Fetal Bovine Serum (FBS), displayed a red shift of the peak wavelength as compared to naked GNPs. This is due to the attachment of serum proteins onto the surface of the GNPs. Our FTIR spectra (see **Figure 2.3C**) displayed the presence of serum proteins on the surface of the NPs. The hydrodynamic radius of the GNPs increased and is shown in the table in **Figure 2.3D**. However, the red shift of the peak wavelength was the same for the GNPs incubated in the normoxic and hypoxic chamber. This indicates that the hypoxic environment does not affect the mono-dispersity of the NPs.

2.3.2 Measurement of Toxicity of GNPs Under Hypoxic Conditions

The toxicity was measured by comparing the cell proliferation rate with and without NPs under both normoxic and hypoxic conditions for over 42 hours. The results are presented in **Figure 2.4** for Hela and MCF-7 cell lines under normoxia and hypoxia. There was no significant reduction in cell proliferation observed for cells treated with GNPs under hypoxia and normoxia, as compared to the control where cells were not treated with GNPs. The concentration of the GNPs used in our experiments was 0.6nMol. The toxicity was also measured for twice the concentration, i.e. 1.2 nMol. There was no significant induced toxicity due to the presence GNPs within the cells. The cell proliferation rate for MCF-7 and HeLa was different.

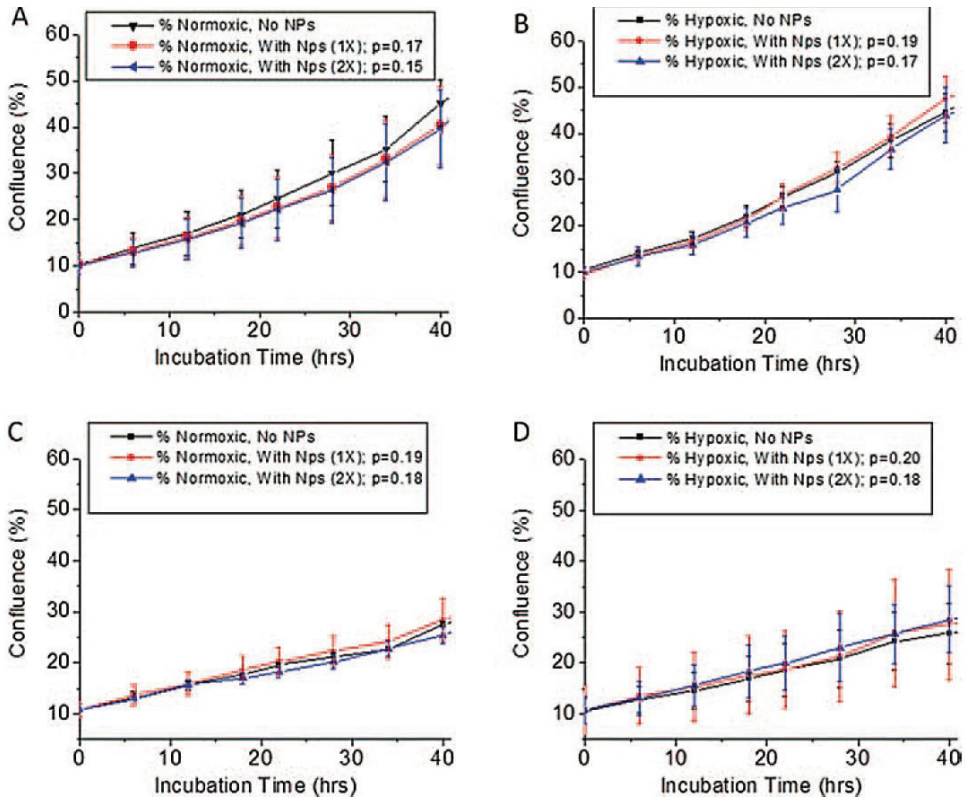

<Figure 2.4> Toxicity evaluation of the GNPs. The toxicity induced by the NPs was measured by monitoring the cell proliferation for HeLa (A)–(B) and MCF-7 (C)–(D) cells in normoxic and hypoxic conditions. The concentration of NPs in the tissue culture media was 0.6 nMol and 1.2 nMol. There was no significant difference in toxicity for cells incubated with NPs under hypoxic and normoxic conditions ($p > 0.05$). Individual statistical significance data (p values) are listed in each graph. The cell proliferation rate was slower for MCF-7 cells compared to HeLa cells due their longer cell doubling time. All results are the mean of three independent experiments ± SE.

2.3.3 Quantitative Analysis of Nanoparticle Uptake under Hypoxia and Normoxia

One of the major objectives of this study was to compare the NP uptake under normoxia and hypoxia. We used both quantitative (AAS) and qualitative (CytoViva hyperspectral imaging) techniques to verify the outcome of our cell uptake studies. Our cell uptake experiments were carried out at a concentration of 0.6 nMol, and the NP uptake per cell was quantified using AAS

technique. As illustrated in **Figure 2.5**, cell uptake of NPs was mainly dependent on the exposure of cells to hypoxic conditions before introducing the NPs. The top and bottom panels of **Figure 2.5** show the GNP uptake data for cells (MCF-7and HeLa) incubated under normoxia and hypoxia for 4 and 18 hours prior to introducing the NPs, respectively. Once NPs were introduced into the tissue culture, we monitored their uptake by cells at 6 and 24 hour time points. At the 6 hour time point, the hopoxic cells had lower uptake than normoxic cells. However, the cells pre-exposed to hypoxia for 4 hours showed lower NP uptake compared to the cells pre-exposed to hypoxia for 18 hours. At the 24 hour time point, the cells pre-exposed to hypoxia for 18 hours showed a higher NP uptake than the cells pre-exposed to hypoxia for 4 hours. In addition, the cells pre-exposed to hypoxia for 18 hours showed higher NP uptake than normoxic cells after incubation with them for 24 hours. One of the major objectives of this study was to compare the NP uptake under normoxia and hypoxia. We used both quantitative (AAS) and qualitative (CytoViva hyperspectral imaging) techniques to verify the outcome of our cell uptake studies. Our cell uptake experiments were carried out at a concentration of 0.6 nMol, and the NP uptake per cell was quantified using AAS technique. As illustrated in **Figure 2.5**, cell uptake of NPs was mainly dependent on the exposure of cells to hypoxic conditions before introducing the NPs. The top and bottom panels of **Figure 2.5** show the GNP uptake data for cells (MCF-7and HeLa) incubated under normoxia and hypoxia for 4 and 18 hours prior to introducing the NPs, respectively. Once NPs were introduced into the tissue culture, we monitored their uptake by cells at 6 and 24 hour time points. At the 6 hour time point, the hopoxic cells had lower uptake than normoxic cells. However, the cells pre-exposed to hypoxia for 4 hours showed lower NP uptake compared to the cells pre-exposed to hypoxia for 18 hours. At the 24 hour time point, the cells pre-exposed to hypoxia for 18 hours showed a higher NP uptake than the cells pre-exposed

to hypoxia for 4 hours. In addition, the cells pre-exposed to hypoxia for 18 hours showed higher NP uptake than normoxic cells after incubation with them for 24 hours.

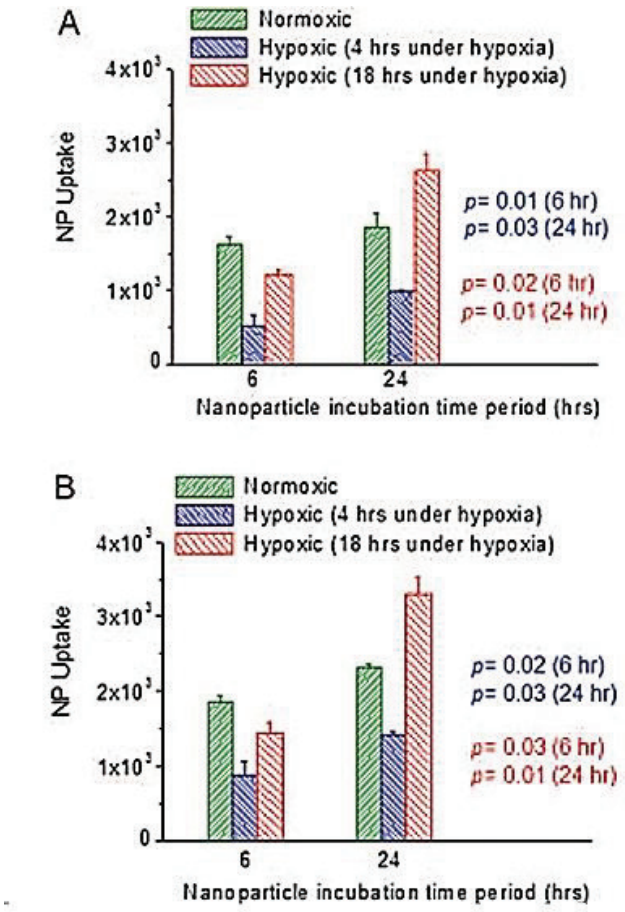

<Figure 2.5> Cellular uptake of GNPs in normoxic and hypoxic cells. (A)–(B) The NP uptake in MCF-7 and HeLa cells that were exposed to hypoxic conditions for 4 and 18 hours prior to NP addition, respectively. The concentration of NPs in the tissue culture media was 0.6 nMol. The hypoxic cells had a lower NP uptake compared to the normoxic cells at the 6-hour NP incubation time point. However, the cells exposed to prolonged (16 hours) hypoxia had a higher NP uptake compared to the normoxic cells at the 24-hour time point. All results are the mean of three independent experiments ± SE. The statistical significance data (p values) are listed in each graph.

2.3.4 Qualitative Analysis of GNPs Distribution Under Hypoxia and Normoxia

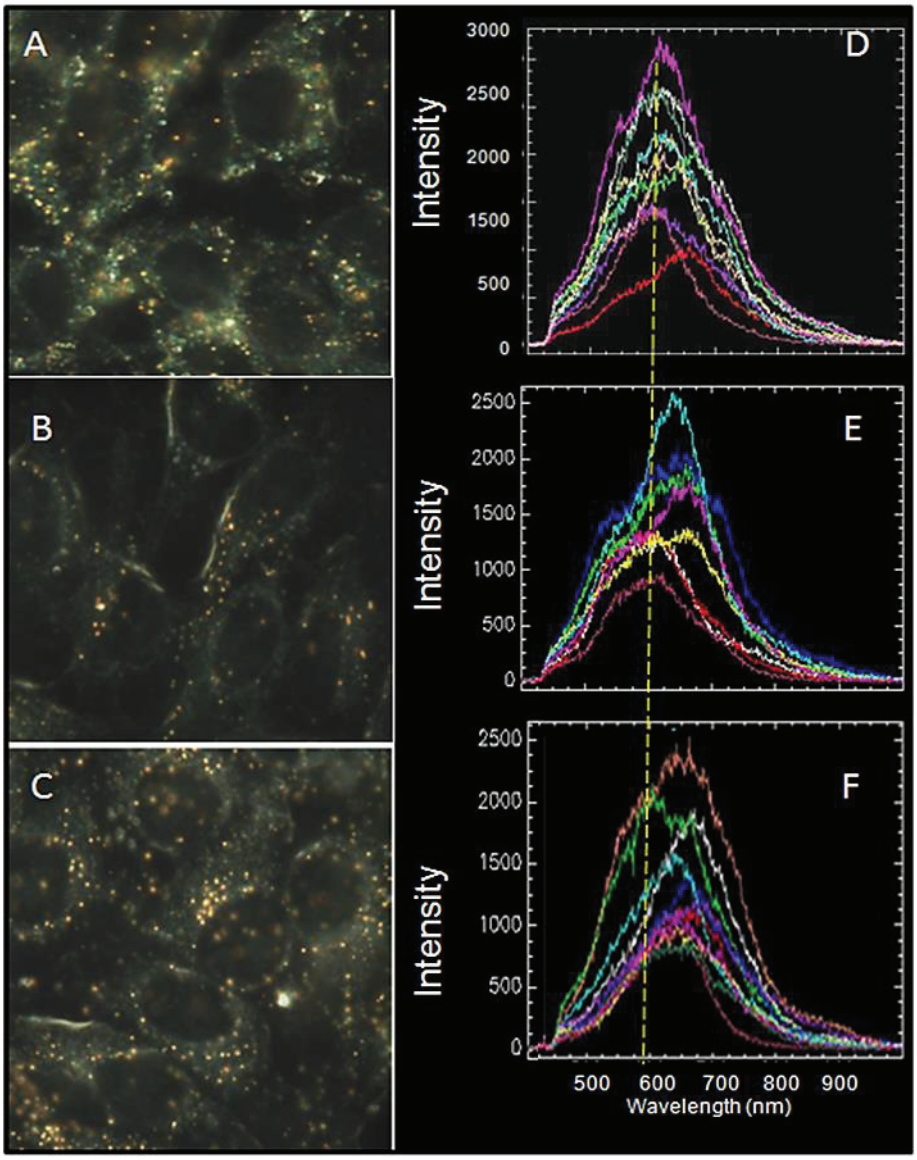

<Figure 2.6> Hyperspectral imaging of GNPs in normoxic and hypoxic cells. (A)–(C) Dark field images of GNPs localized in normoxic, hypoxic (4 hours in the chamber before introducing NPs), and hypoxic (18 hours in the chamber before introducing NPs) cells after 24 hours of incubation with NPs. (D)–(F) Reflectance spectra from ten GNP clusters localized in the cells shown in images (A)–(C), respectively.

For qualitative analysis of NP uptake, we used the hyperspectral imaging technique. With the integrated CytoViva hyperspectral imaging capability, reflectance spectra from GNPs can be captured. This spectral image analysis capability also enables the ability to differentiate NPs that

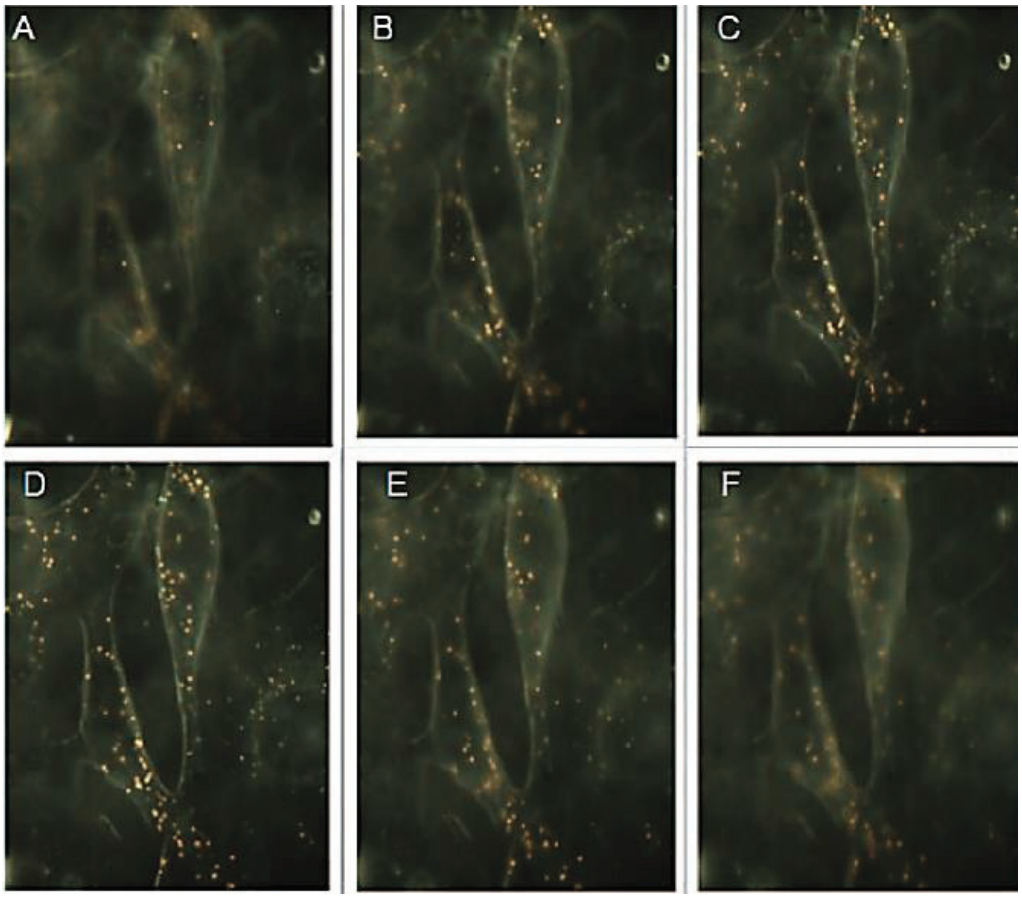

<Figure 2.7> A panel of images to visualize the GNP distribution within different planes of the cells pre-exposed to hypoxia for eighteen hours followed by incubation with GNPs for twenty-four hours. The images from (A)-(F) are different planes along the Z-axis (assuming that the cells are adhered in the X–Y plane of the cover slip). These planes are approximately 800 nm apart.

are very similar based on minute differences in aggregation, orientation, and function of their surface chemistry within a sample. The dark field images in **Figures 2.6 A-C** display the differences in cellular uptake of GNPs following a 24 hour incubation time period in normoxic cells and in cells pre-exposed to hypoxia for 4 and 18 hours, respectively. With the integrated

CytoViva hyperspectral imaging capability, reflectance spectra from GNP clusters within the cell were captured. The **Figures 2.6 D-F** illustrates the spectral information from 10 GNP clusters selected from images in the corresponding left panel. There is an overall red shift in the spectra collected from hypoxic cells as compared to normoxic cells. **Figure 2.7** shows a detailed analysis of the NP distribution following an incubation time period of 24 hours in cells pre-exposed to hypoxia for 18 hours. The images from A to F were different planes along the Z-axis (assuming that the cells are adhered in the X-Y plane of the cover slip). These planes are approximately 800 nm apart.

2.3.5 Statistical Analysis

Data was obtained from 3 parallel experiments and is expressed as mean ± standard deviation (S.D.). Each experiment was repeated 3 times to check the reproducibility.

2.4 Discussion

It has been shown that the low levels of oxygenation, or hypoxia, commonly present in solid tumors protects cells from death by irradiation.[39] For example, damage to DNA is created by direct ionization from radiation or is induced by the interaction with free radicals (e.g., a hydroxyl radical) formed by the ionization of water surrounding the DNA. If oxygen is available, it can react with the broken ends of the DNA, thereby creating stable organic peroxides. This type of DNA damage cannot easily be repaired. However, the damage is more readily repairable in the absence of molecular oxygen, which would lead to less damage following radiation or chemotherapy [40, 41]. One of the reasons for cancer reoccurrence is that these hypoxic cells can survive this treatment. GNPs are being explored to overcome the resistance by these hypoxic cells because they can be used in combination with radiation therapy and chemotherapy [3.

However; it is unknown how the GNP-based therapeutic response would vary in a real tumor where hypoxia is present. To use GNPs for improved cancer therapeutics, it is necessary to understand their behavior under hypoxia. Previous experimental and theoretical studies have shown that GNPs 50 nm in size have the highest uptake and radiation dose enhancement in properly oxygenated cells. Hence, 50 nm GNPs were used for this study. Initially, the NP stability was investigated by incubating the NPs in media supplemented with FBS for 24 hours under hypoxia and normoxia. The peak wavelength of the UV absorption spectrum was red shifted compared to naked GNPs (**see Figure 2.3 (B)**). However, there was no apparent difference in the red shift for the GNPs incubated under normoxic and hypoxic conditions. The red shift resulted from the binding of the serum proteins in the media onto the GNP surface. As illustrated in **Figure 2.3 (C)**, the presence of serum proteins on the GNP surface was confirmed by the FTIR spectrum. Furthermore, the DLS measurements showed an increase in the hydrodynamic radius for NPs incubated in the media **(Figure 2.3 (D)**).Based on the UV and DLS data, there was no apparent aggregation of the GNPs once exposed to hypoxia for a 24-hour period. This result was an important step towards understanding the variation in toxicity and uptake of GNPs once incubated with cells. It has been shown that GNPs are not toxic to properly oxygenated cells [42]. The variation in cell proliferation was monitored to measure the NP-induced toxicity under hypoxia and normoxia (control) for over 42 hours **(see Figure 2.4)**. The proliferation rate was higher for the HeLa cell line compared to MCF-7. This finding could be due to their difference in cell doubling time. The doubling time measured for the HeLa cell line was approximately 24 hours while it was 48 hours for the MCF-7 cell line. However, there was a statistically significant difference in the cell proliferation rates for cells under hypoxia and normoxia. We also used twice the concentration of GNPs that we normally use for our NP cell

uptake experiments. There was no apparent toxicity induced by GNPs under hypoxia after 42 hours. The NP uptake in cells was dependent two factors: (a) the length of pre-exposure to hypoxia (4 and 18 hours), and (b) the duration of NP incubation (6 and 24 hours) in tissue culture. At the 6-hour NP incubation time point, the hypoxic cells had a lower NP uptake compared to the normoxic cells. This outcome is consistent with previously published data [36]. However, the effect of NP uptake in cells exposed to hypoxia for a longer period of time is not yet known. In this study, we exposed the cells to hypoxia for 18 hours prior to their incubation with NPs. At the 24-hour NP incubation time point, the hypoxic cells pre-exposed to hypoxia for prolonged time (18 hours) had a higher NP uptake than even the normoxic cells. The hypoxic cells with prolonged pre-exposure to hypoxia had a higher NP uptake at both the 6- and 24-hour NP incubation time points, as illustrated in **Figure 2.5**. These differences in NP uptake could be explained by considering the extent of certain cellular processes, such as endocytosis, exocytosis, and autophagy. It is known that NP cell uptake and removal takes place via energy dependent endo-lyso path.[31, 32, 43] . Most of these NPs are taken up by the endocytosis process [31]. Once the NPs enter the cells, they are trapped in the endosomes before being fused with lysosomes for processing. Once processed, these NPs are excreted from the cell through the exocytosis process. Both of the endocytosis and exocytosis processes are energy dependent [44–46]. The normoxic cells achieve equilibrium between the endocytosis and exocytosis processes following 6 to 8 hours of incubation with NPs. Hence, the increase in NP uptake from a 6-hour time point to a 24-hour time point in normoxic cells was not statistically significant [31]. The cells pre-exposed to hypoxia for 4 and 18 hours showed a lower NP uptake at the 6-hour time point. As previously mentioned, the intracellular NP uptake and transport processes are energy dependent. However, hypoxic cells have limited O2, and only 2ATP molecules are generated per glucose molecule (anaerobic

glycolysis). This process is explained in **Figure 2.1**. A normoxic cell can generate 36 ATP molecules per glucose molecule. Hence, lower NP uptake in hypoxic cells compared to normoxic cells could be due to the presence of less energy available at the cellular level. Our results are consistent with the previous study by Jain et al.[36] The lower NP uptake may be due to a reduction in the endocytosis process.[36] However, the reason for lower NP uptake in cells exposed to hypoxia for a shorter period of time (four hours) is not yet fully known. The NP uptake in cells pre-exposed to hypoxia for 18 hours was higher than the cells pre-exposed to hypoxia for 4 hours at the 6- and 24-hour NP incubation time points. The NP uptake in cells pre-exposed to hypoxia for a longer period of time (18 hours) was higher than the cells pre-exposed to hypoxia for a shorter period of time (4 hours) at the 6- and 24-hour NP incubation time points. This increased presence of NPs in cells exposed to prolonged hypoxia is not yet fully understood. Previous publications have shown that longer exposure of cells to hypoxic conditions could lead to reduced nutrients and energy supply. The autophagy process is stimulated as a result of the reduced nutrient availability.[28, 29] In addition, exocytosis is also further reduced to conserve cellular constituents and energy once the autophagy process begins.[47–49] Reduction in the exocytosis process may result in accumulation of NPs overtime within hypoxic cells. However, more experiments are necessary to fully elucidate the mechanisms of endocytosis and exocytosis of NPs in hypoxic cells. An increase in the presence of aggregated NPs within the hypoxic cells compared to normoxic cells was also observed. There was an overall red shift of the GNP reflectance spectra, as illustrated in **Figure 2.5**. This shift could be due to the increased acidic conditions in the hypoxic cells as a result of an increased presence of lactic acid produced during energy production [50]. This study illustrated that NP uptake was higher in cells that were under hypoxic conditions for a lengthy period of time. The increased number of NPs within the

hypoxic cells could be used to deliver a higher therapeutic load to overcome drug and radiation resistance. Hence, a more aggressive combined approach could be applied because GNPs could be used as both a drug carrier and radiation dose enhancer [3]. Furthermore, recent developments have shown successful incorporation of GNPs into polymer- and lipid-based NPs [4]. This incorporation will allow for the targeting of NP therapeutics into tumors using their leaky vasculature and thus reduce the toxicity to healthy cells. This study provides information as to how NP stability, toxicity, and uptake vary in a real tumor-like hypoxic environment. Hence, these findings will play a critical role in the use of NPs in future cancer therapeutics. Our future goal is to investigate the efficacy of such GNP-based treatments in a hypoxic environment. Proper understanding of NP behavior and the therapeutic response in a tumor-like environment (hypoxic) can be used to improve the outcome of future cancer care [3]. The biocompatibility of GNPs would accelerate the application of such innovations to clinics in the near future [42–44].

2.5 Conclusions

Our studies showed that the GNPs were stable under hypoxic and normoxic conditions following 24 hours of incubation in FBS-supplemented media. Next, we investigated the NP toxicity in MCF-7 and HeLa cell lines under normoxic and hypoxic conditions. Based on the cell proliferation data, there was no apparent toxicity from the presence of GNPs under hypoxic and normoxic conditions for both cell lines. Finally, we evaluated the NP uptake in hypoxic and normoxic cells. Our results showed that NP uptake was dependent on the duration of the time that cells were exposed to hypoxic conditions before introducing GNPs. Cells that were pre-exposed to hypoxia for 4 hours prior to NP incubation showed a lower uptake following 24 hours of incubation with NPs. In contrast, cells that were pre-exposed to hypoxia for 18 hours showed a higher uptake after 24 hours of incubation with NPs. Based on our NP characterization data

(Figure 2.2), there was no significant change in the NP features following incubation under hypoxic conditions. Hence, the observed difference in NP uptake under hypoxia was independent of NP features. The observed difference in NP uptake in hypoxic cells could be due to a combination of many processes, such as endocytosis, exocytosis, and autophagy, occurring at different rates based on the energy availability at the cellular level.

Acknowledgments

The authors would like to acknowledge the Natural Sciences and Engineering Research Council of Canada (NSERC), the Canadian Foundation for Innovation and Ryerson University for their financial support. The authors would like to thank Dr. Richard P. Hill, Dr. Robert G. Bristow, and Dr. Bradly G. Wouters at the Ontario Cancer Institute for their valuable research support and guidance.

2.6 Notes and References

[1]Department of Physics, Ryerson University, 350 Victoria Street, Toronto, ON, M5B 2K3, Canada
[2]Ontario Cancer Institute, Toronto Medical Discovery Tower, Toronto, ON, M5G 1L7, Canada

1. Chithrani, D. B. (2010). Intracellular uptake, transport, and processing of gold nanostructures. *Molecular membrane biology*, *27*(7), 299-311.

2. Chithrani, D. B. (2011). Optimization of bio-nano interface using gold nanostructures as a model nanoparticle system. *Insciences Journal.*, *1*(3), 115-135.

3. Jelveh, S., & Chithrani, D. B. (2011). Gold nanostructures as a platform for combinational therapy in future cancer therapeutics. *Cancers*, *3*(1), 1081-1110.

4. B Chithrani, D. (2010). Nanoparticles for improved therapeutics and imaging in cancer therapy. *Recent patents on nanotechnology*, *4*(3), 171-180.

5. Cuenca, A. G., Jiang, H., Hochwald, S. N., Delano, M., Cance, W. G., & Grobmyer, S. R. (2006). Emerging implications of nanotechnology on cancer diagnostics and therapeutics. *Cancer*, *107*(3), 459-466.

6. Rao, J. (2008). Shedding light on tumors using nanoparticles. *ACS nano*, *2*(10), 1984-1986.

8. Chithrani, D. B., Jelveh, S., Jalali, F., van Prooijen, M., Allen, C., Bristow, R. G, Jaffray, D. A. (2010). Gold nanoparticles as radiation sensitizers in cancer therapy. *Radiation research*, *173*(6), 719-728.

9. Hainfeld, J. F., Slatkin, D. N., & Smilowitz, H. M. (2004). The use of gold nanoparticles to enhance radiotherapy in mice. *Physics in medicine and biology*, *49*(18), N309.

10. Jain, S., Hirst, D. G., & O'sullivan, J. M. (2014). Gold nanoparticles as novel agents for cancer therapy. *The British Journal of Radiology, 85*(1010), 101-113

11. D. B. Chithrani (2013), Cancer Nanotechnology: Principles and Applications in Radiation Oncology, edited by S. H. K. Cho, S., CRC Press, Boca Raton, 1, 111-122.

12. Yang, C., Neshatian, M., van Prooijen, M., & Chithrani, D. B. (2014). Cancer Nanotechnology: Enhanced Therapeutic Response Using Peptide-Modified Gold Nanoparticles. *Journal of nanoscience and nanotechnology*, *14*(7), 4813-4819.

13. Vaupel, P., F. Kallinowski, and P. Okunieff. (1990). Blood flow, oxygen consumption and tissue oxygenation of human tumors. Oxygen Transport to Tissue XII. Springer US, 895-905.

14. Liao, D., & Johnson, R. S. (2007). Hypoxia: a key regulator of angiogenesis in cancer. *Cancer and Metastasis Reviews*, *26*(2), 281-290.

15. Vaupel, P. (2004). The role of hypoxia-induced factors in tumor progression. *The oncologist*, *9*(Supplement 5), 10-17.

16.Carmeliet, P., & Jain, R. K. (2000). Angiogenesis in cancer and other diseases. *nature*, *407*(6801), 249-257.

17. Torres Filho, I. P., Leunig, M., Yuan, F., Intaglietta, M., & Jain, R. K. (1994). Noninvasive measurement of microvascular and interstitial oxygen profiles in a human tumor in SCID mice. *Proceedings of the National Academy of Sciences*, *91*(6), 2081-2085.

18. Helmlinger, G., Yuan, F., Dellian, M., & Jain, R. K. (1997). Interstitial pH and pO2 gradients in solid tumors in vivo: high-resolution measurements reveal a lack of correlation. *Nature medicine*, *3*(2), 177-182.

19. Primeau, Andrew J., et al. 2005, The distribution of the anticancer drug Doxorubicin in relation to blood vessels in solid tumors. *Clinical Cancer Research*, 11(24): 8782-8788.

20. Vaupel, P., Schlenger, K., Knoop, C., & Höckel, M. (1991). Oxygenation of human tumors: evaluation of tissue oxygen distribution in breast cancers by computerized O2 tension measurements. *Cancer research*, *51*(12), 3316-3322.

21. Brown, J. M., & Wilson, W. R. (2004). Exploiting tumour hypoxia in cancer treatment. *Nature Reviews Cancer*, *4*(6), 437-447.

22. Chan, N., Koch, C. J., & Bristow, R. G. (2009). Tumor hypoxia as a modifier of DNA strand break and cross-link repair. *Current molecular medicine*, *9*(4), 401-410.

23. Bristow, R. G., & Harrington, L. (Eds.). (1998). *The basic science of oncology* (pp. 135-165). New York: McGraw-Hill.

24. Luoto, K. R., Kumareswaran, R., & Bristow, R. G. (2013). Tumor hypoxia as a driving force in genetic instability. *Genome integrity*, *4*(5), 1-15.

25. Cairns, R. A., Harris, I. S., & Mak, T. W. (2011). Regulation of cancer cell metabolism. *Nature Reviews Cancer*, *11*(2), 85-95.

26. Seagroves, T. N., Ryan, H. E., Lu, H., Wouters, B. G., Knapp, M., Thibault, P, Johnson, R. S. (2001). Transcription factor HIF-1 is a necessary mediator of the pasteur effect in mammalian cells. *Molecular and cellular biology*, *21*(10), 3436-3444.

27. Gillies, R. J., Robey, I., & Gatenby, R. A. (2008). Causes and consequences of increased glucose metabolism of cancers. *Journal of Nuclear Medicine*, *49*(Suppl 2), 24S-42S.

28. Takagi, H., King, G. L., & Aiello, L. P. (1998). Hypoxia upregulates glucose transport activity through an adenosine-mediated increase of GLUT1 expression in retinal capillary endothelial cells. *Diabetes*, *47*(9), 1480-1488.

29. Ouiddir, A., Planès, C., Fernandes, I., VanHesse, A., & Clerici, C. (1999). Hypoxia upregulates activity and expression of the glucose transporter GLUT1 in alveolar epithelial cells. *American journal of respiratory cell and molecular biology*, *21*(6), 710-718.

30. Chithrani, B. D., Stewart, J., Allen, C., & Jaffray, D. A. (2009). Intracellular uptake, transport, and processing of nanostructures in cancer cells. *Nanomedicine: Nanotechnology, Biology and Medicine*, *5*(2), 118-127.

31. Chithrani, B. D., Ghazani, A. A., & Chan, W. C. (2006). Determining the size and shape dependence of gold nanoparticle uptake into mammalian cells. *Nano letters*, *6*(4), 662-668.

32. Gao, H., Shi, W., & Freund, L. B. (2005). Mechanics of receptor-mediated endocytosis. *Proceedings of the National Academy of Sciences of the United States of America*, *102*(27), 9469-9474.

33. Zhang, S., Li, J., Lykotrafitis, G., Bao, G., & Suresh, S. (2009). Size-Dependent Endocytosis of Nanoparticles. *Advanced Materials*, *21*(4), 419-424.

34. Aoyama, Y., Kanamori, T., Nakai, T., Sasaki, T., Horiuchi, S., Sando, S., & Niidome, T. (2003). Artificial viruses and their application to gene delivery. Size-controlled gene coating with glycocluster nanoparticles. *Journal of the American Chemical Society*, *125*(12), 3455-3457.

35. Jiang, W., Kim, B. Y., Rutka, J. T., & Chan, W. C. (2008). Nanoparticle-mediated cellular response is size-dependent. *Nature nanotechnology*, *3*(3), 145-150.

36. Jain, S., Coulter, J. A., Hounsell, A. R., Butterworth, K. T., McMahon, S. J., Hyland, W.B.Hirst, D. G. (2011). Cell-specific radiosensitization by gold nanoparticles at megavoltage radiation energies. *International Journal of Radiation Oncology Biology Physics*, *79*(2), 531-539.

37. Frens, G. (1973). Controlled nucleation for the regulation of the particle size in monodisperse gold suspensions. *Nature*, *241*(105), 20-22.

38. S. O. P. Cristiana, M. M. Lino, A. A. Matos, and L. S. Ferreira, (2013). Differential internalization of amphotericin B e conjugated nanoparticles in human cells and the expression of heat shock protein. *Biomaterial*. 70, 34-5281.

39. Moeller, B. J., Richardson, R. A., & Dewhirst, M. W. (2007). Hypoxia and radiotherapy: opportunities for improved outcomes in cancer treatment. *Cancer and Metastasis Reviews*, *26*(2), 241-248.

40. Dische, S., Anderson, P. J., Sealy, R., & Watson, E. R. (1983). Carcinoma of the cervix—anaemia, radiotherapy and hyperbaric oxygen. *The British journal of radiology*, *56*(664), 251-255.

41. Sullivan, R., Paré, G. C., Frederiksen, L. J., Semenza, G. L., & Graham, C. H. (2008). Hypoxia-induced resistance to anticancer drugs is associated with decreased senescence and requires hypoxia-inducible factor-1 activity. *Molecular cancer therapeutics*, *7*(7), 1961-1973.

42. Shukla, R., Bansal, V., Chaudhary, M., Basu, A., Bhonde, R. R., & Sastry, M. (2005). Biocompatibility of gold nanoparticles and their endocytotic fate inside the cellular compartment: a microscopic overview. *Langmuir*, *21*(23), 10644-10654.

43. Chithrani, B. D., & Chan, W. C. (2007). Elucidating the mechanism of cellular uptake and removal of protein-coated gold nanoparticles of different sizes and shapes. *Nano letters*, *7*(6), 1542-1550.

44 Hu, L., Mao, Z., Zhang, Y., & Gao, C. (2011). Influences of size of silica particles on the cellular endocytosis, exocytosis and cell activity of HepG2 cells. *Journal of Nanoscience Letters| Volume*, *1*(1), 1-16.

45. Tormena, C. F., Lacerda Jr, V., & Oliveira, K. T. D. (2010). Revisiting the Stability of endo/exo Diels-Alder Adducts between Cyclopentadiene and 1, 4-benzoquinone. *Journal of the Brazilian Chemical Society*, *21*(1), 112-118.

46. Panyam, J., & Labhasetwar, V. (2003). Dynamics of endocytosis and exocytosis of poly (D, L-lactide-co-glycolide) nanoparticles in vascular smooth muscle cells. *Pharmaceutical research*, *20*(2), 212-220.

47. H. Shorer, N. Amar, A. Meerson, and Z. (2005). Elazar, Modulation of N-ethylmaleimidesensitive factor activity upon amino acid deprivation. *Jornal of Biological. Chemistry.* 280, 16219.

48. Bellot, G., Garcia-Medina, R., Gounon, P., Chiche, J., Roux, D., Pouysségur, J., & Mazure, N. M. (2009). Hypoxia-induced autophagy is mediated through hypoxia-inducible factor induction of BNIP3 and BNIP3L via their BH3 domains. *Molecular and cellular biology*, *29*(10), 2570-2581.

49. X Ma, X., Wu, Y., Jin, S., Tian, Y., Zhang, X., Zhao, Y., ... & Liang, X. J. (2011). Gold nanoparticles induce autophagosome accumulation through size-dependent nanoparticle uptake and lysosome impairment. *ACS nano*, *5*(11), 8629-8639.

50. Tannock, I. F., & Rotin, D. (1989). Acid pH in tumors and its potential for therapeutic exploitation. *Cancer research*, *49*(16), 4373-4384.

3 Summary and Future Work

3.1 Summary

The purpose of this project was to investigate the toxicity and uptake of GNPs under hypoxic conditions. GNPs of size 50 nm were incubated in HeLa and MCF-7 cancer cells under normal oxygen tension (21% O_2) and hypoxic oxygen tension (0.2% O_2). Our study showed that GNPs were stable in tissue culture media under normoxic and hypoxic conditions after 24 hours incubation. Cell proliferation rate was monitored to investigate the cellular toxicity under hypoxia and normoxia. There was no induced cellular toxicity due to GNPs. Uptake of GNPs under hypoxic and normoxic condition was studied for the above-mentioned cell lines using 50 nm GNPs. Our results showed that the number of GNPs internalized within a cell was dependent on the duration of exposure of cells under hypoxia before introducing NPs. Cells exposed to prolonged hypoxia (18 hours) had a higher NP uptake as compared to ones exposed to shorter period of time (4 hours).

3.2 Future Studies

Introduction

The ultimate goal in cancer therapy is to target cancer cells and deliver a maximum dose of anticancer drugs and radiation dose while causing a minimum damage to normal tissues. Among other NP-based therapeutics, GNP-based approaches are more favorable due to their ability to act as a drug delivery vehicle and a radiosensitizer in cancer therapy [1-3].

Previous studies have shown that the size of GNPs is a crucial factor in their uptake. It has been shown that 50 nm GNPs have the highest uptake and radiation dose enhancement [4, 5]. However, these studies were performed using proper oxygenated (normoxic) cancer cells. It has been

shown most of the solid tumors have hypoxic regions and those regions are mostly responsible for radiation and/or chemotherapy resistance [6-13]. Hence, it is important to understand the uptake of GNPs in real tumor environment, such as hypoxic, to fully exploit their potential in cancer therapy applications. A recent study has shown that the uptake of NPs was dependent on the level of hypoxia within those cells In that study cells which were exposed to prolonged hypoxia showed higher uptake for 50nm GNPs as compared to the cells exposed to hypoxia for a shorter period of time [14]. However, we still do not know how the size of the NPs affects their cellar uptake and radiation dose enhancement under hypoxic conditions.

3.3 Size Dependent Uptake of GNPs in Hypoxic Cells

Methodology

3.3.1 GNPs Synthesis and Characterization

GNPs of size 15nm, 50nm and 70nm were synthesized using the citrate reduction method [15]. In this method, 300 ml of 1% $HAuCl_4.3H_2O$ was added to 30 ml of double-distilled water and heated to boil while stirring. Once it started boiling, 120, 300 and 500 µl of 1% sodium citrate tribasic was added to the solution and kept stirring for another 5 minutes. The mixture was brought to room temperature while stirring. GNPs were characterized using UV-Visible spectroscopy, DLS, and TEM imaging.

3.3.2 Cell culture

We used a breast cancer cell line (MCF-7) and a cervical cancer cell line (HeLa) for our study. The cells were cultured in Dulbecco's modified Eagle's medium (DMEM) supplemented with 10% FBS. Cells were incubated at 37°C in a humidified incubator with 95% air/5% CO_2. For cellular uptake studies, the cells were grown in petri dishes (100 mm x 15 mm) until they

reached 80% confluency and incubated with fresh tissue culture medium prior to each incubation experiment with NPs in either normoxic or hypoxic conditions.

3.3.3 Cell Uptake

Cells were seeded with 2.2 $\times 10^6$ density in 10 cm tissue culture dishes. When they reached 80% confluence, half of the dishes were moved to the hypoxia chamber and the rest were left in a regular normoxic incubator. The cells and GNP solutions were kept in the hypoxia chamber separately to reach hypoxic conditions. The hypoxia chamber was set at 0.2% O_2. We used the following timeline for our study.

1. Cells were in hypoxia chamber for 4 hours prior to NP addition. GNPs were incubated for 6 and 24 hours before processing them for quantification studies.
2. Cells were in hypoxia chamber for 18 hours prior to NP addition. GNPs were incubated for 6 and 24 hours before processing them for quantification studies.

3.3.4 Quantification

After NP incubation, cells were washed three times with Phosphate Buffered Saline (PBS) to wash unbound GNPs and trypsin was added to detached cells from the petri dish. Cell were counted and processed at 120°C in nitric acid for a half hour for quantification using Inductively Coupled Plasma Atomic Absorption Spectroscopy (ICP-AES) technique.

3.3.5 Cellular Toxicity

HeLa and MCF-7 cells (0.02×10^6) were seeded in 24-well dishes. Once cells were adhered to the tissue culture dishes, one set of dishes and a suspension of GNPs were transferred to the hypoxia chamber while the other set was left in the normoxic chamber. After 4 hours, GNPs were added to the one set of dishes in the normoxic and hypoxic chambers. The concentration of GNPs used

was 0.6 and 1.2 nMol. Kinetic Live Cell Imaging System (IncuCyte™) was used to monitor cell proliferation pattern. The device recorded the cell proliferation data every two hours over 48 hours.

3.4 Preliminary Results and Discussion

3.4.1 Characterization of GNPs

GNPs were characterized using UV-Vis spectroscopy, DLS and TEM imaging. The stability of GNPs was tested under normoxic and hypoxic conditions by keeping them in respective chambers for 24 hours. Results are shown in **Table. 3.1** and there was no apparent aggregation of GNPs.

<Table. 3.1> Characterization of colloidal GNPs. Hydrodynamic diameter and UV visible peak wavelength of as-made GNPs and GNPs incubated with FBS supplemented media for duration of 24 h under normoxic and hypoxic (0.2% O_2) conditions, respectively

Diameter of GNPs TEM (nm)	As made GNPs (Hydrodynamic diameter) (nm)	GNPs incubated in normoxic chamber (Hydrodynamic diameter) (nm)	GNPs incubated in hypoxic chamber (Hydrodynamic diameter) (nm)
15	18 .3 ± 4.3	23.2 ± 3.1	24.1 ± 4.6
50	55.2 ± 5.5	61.8 ± 6.1	61.2 ± 5.6
70	76.4 ± 7.2	80.7 ± 6.8	81.2± 7.3

3.4.2 Measurement of Toxicity of GNPs Under Hypoxic

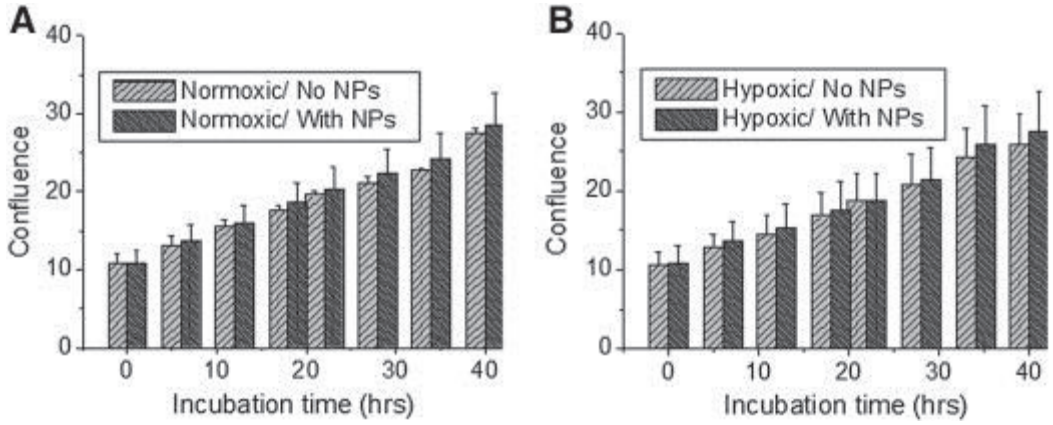

<Fig. 3.1> Evaluation of the toxicity of GNPs. (A)–(B) The toxicity induced by GNPs was measured by monitoring cell proliferation for MCF-7 cells in normoxic and hypoxic conditions, respectively. The concentration of NPs used was 0.6 nMol. The results are the mean of three independent experiments ± SE.

Confluence of cells incubated with and without GNPs under hypoxic and normoxic conditions for 48 hours are shown in **Figure 3.1**. There was no significant difference in cell proliferation for cells incubated with NPs as compared to control cells with no NPs under hypoxic and normoxic conditions.

3.4.3 Size Dependent GNP Uptake Under Hypoxic and Normoxic Conditions

Preliminary results showed GNP uptake in hypoxic cells was size dependent and GNPs of diameter 50nm have the highest uptake (**Figure 3.2**). Cells exposed to prolonged hypoxia showed higher uptake for all three sizes. One of the future studies will be to evaluate the variation in radiation dose enhancement due to GNPs under hypoxic conditions for different size NPs.

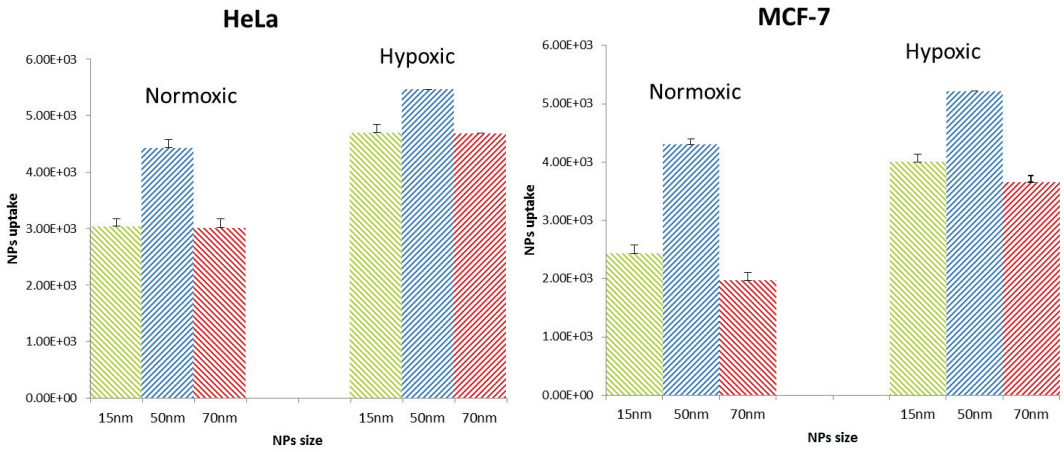

<Fig3.2> Quantitative results for GNPs uptake in hypoxic and Normoxic cells. The cells exposed to prolong (18 hours) hypoxia had a higher NP uptake as compared to normoxic cells. Among NPs of sizes 15, 50, and 70 nm, NPs of diameter 50 nm had the highest uptake under both normoxic and hypoxic conditions. The results are the mean of three independent experiments ± SE.

3.4.4 Discussion

GNPs uptake and toxicity to cells exposed to prolong hypoxia was investigated. Results showed GNPs of different sizes were stable in the media both in hypoxic and normal oxygen tension. It was also shown that GNPs of different sizes were not toxic to hypoxic cells or normoxic cells. Uptake results showed prolong hypoxia associates with higher accumulation of GNPs in the cells. This can be due to autophagy process in cells exposed to prolong hypoxia which can further reduces exocytosis process and results in accumulation of GNPs in the cells. However, more detail study should be done in the mechanism of GNPs transportation within the hypoxic cells to elucidate these findings. Also uptake in hypoxic cells was size dependent and the optimum size for maximum uptake in the cells was 50 nm. Future study should be done to elucidate if combination of GNPs and radiation and/or chemotherapy can be overcome the therapeutic resistance in hypoxic cells.

3.5 References

1. Jelveh, S., & Chithrani, D. B. (2011). Gold nanostructures as a platform for combinational therapy in future cancer therapeutics. *Cancers*, *3*(1), 1081-1110.

2. Chithrani, D. B. (2011). Optimization of bio-nano interface using gold nanostructures as a model nanoparticle system. *Insciences J.*, *1*(3), 115-135.

3. Jain, S., Hirst, D. G., & O'sullivan, J. M. (2014). Gold nanoparticles as novel agents for cancer therapy. The British Journal of Radiology, 85(1010) , 101-113.

4. Chithrani, B. D., Ghazani, A. A., & Chan, W. C. (2006). Determining the size and shape dependence of gold nanoparticle uptake into mammalian cells. *Nano letters*, *6*(4), 662-668.

5. Zhang, S., Li, J., Lykotrafitis, G., Bao, G., & Suresh, S. (2009). Size-Dependent Endocytosis of Nanoparticles. *Advanced Materials*, *21*(4), 419-424.

6. Moeller, B. J., Richardson, R. A., & Dewhirst, M. W. (2007). Hypoxia and radiotherapy: opportunities for improved outcomes in cancer treatment. *Cancer and Metastasis Reviews*, *26*(2), 241-248.

7. Thomlinson, R. H., & Gray, L. H. (1955). The histological structure of some human lung cancers and the possible implications for radiotherapy. *British journal of cancer*, *9*(4), 539-549.

8. Brown, J. M. (2000). Exploiting the hypoxic cancer cell: mechanisms and therapeutic strategies. *Molecular medicine today*, *6*(4), 157-162.

9. Harrison, L. B., Chadha, M., Hill, R. J., Hu, K., & Shasha, D. (2002). Impact of tumor hypoxia and anemia on radiation therapy outcomes. *The Oncologist*, *7*(6), 492-508.

10. Yoshiba, S., Ito, D., Nagumo, T., Shirota, T., Hatori, M., & Shintani, S. (2009). Hypoxia induces resistance to 5-fluorouracil in oral cancer cells via G1 phase cell cycle arrest. *Oral oncology*, *45*(2), 109-115.

11. Teicher, B. A., Lazo, J. S., & Sartorelli, A. C. (1981). Classification of antineoplastic agents by their selective toxicities toward oxygenated and hypoxic tumor cells. *Cancer research*, *41*(1), 73-81.

12. Gerweck, L. E., Kozin, S. V., & Stocks, S. J. (1999). The pH partition theory predicts the accumulation and toxicity of doxorubicin in normal and low-pH-adapted cells. *British journal of cancer*, *79*(5-6), 838-842.

13. Wang, F., Wang, Y. C., Dou, S., Xiong, M. H., Sun, T. M., & Wang, J. (2011). Doxorubicin-tethered responsive gold nanoparticles facilitate intracellular drug delivery for overcoming multidrug resistance in cancer cells. *ACS nano*, *5*(5), 3679-3692.

14. Neshatian Mehrnoosh, Chung Stephen, Yohan Darren, Yang Celina, Chithrani Devika. Uptake of gold nanoparticles in breathless (hypoxic) Cancer cells. (2015) *Journal of Biomedical Nanotechnology,* in press.

15. Frens, G. (1973). Controlled nucleation for the regulation of the particle size in monodisperse gold suspensions. *Nature*, *241*(105), 20-22.

16. Shorer, H., Amar, N., Meerson, A., & Elazar, Z. (2005). Modulation of N-ethylmaleimide-sensitive factor activity upon amino acid deprivation. *Journal of Biological Chemistry*, *280*(16), 16219-16226.